

Adfreeze strength of Wooden Piles in Warm Permafrost Soil

John McLean¹, Ali Saeidi^{2*}, Rama Vara Prasad Chavali³, Mahdiyeh Seifaddini⁴, Andreeanne Clement⁵,
Thomas Barbarisque⁶, Jean-Pascal Bilodeau⁷

¹MSc student, Département des Sciences Appliquées, Université du Québec à Chicoutimi, Chicoutimi, QC, G7H 2B1, Canada. Email: john-jr.mc-lean1@uqac.ca

^{2*}Professor, Département des Sciences Appliquées, Université du Québec à Chicoutimi, Chicoutimi, QC, G7H 2B1, Canada. Email: Ali_Saeidi@uqac.ca

³Postdoctoral Researcher, Département des Sciences Appliquées, Université du Québec à Chicoutimi, Chicoutimi, QC, G7H 2B1, Canada. Email: Rama-vara-prasad.chavali1@uqac.ca

⁴Researcher, Département des Sciences Appliquées, Université du Québec à Chicoutimi, Chicoutimi, QC, G7H 2B1, Canada. Email: Mahdiyeh_Seifaddini@uqac.ca

⁵MSc student, Département des Sciences Appliquées, Université du Québec à Chicoutimi, Chicoutimi, QC, G7H 2B1, Canada. Email: andreeanne.clement1@uqac.ca

⁶MSc student, Département des Sciences Appliquées, Université du Québec à Chicoutimi, Chicoutimi, QC, G7H 2B1, Canada. Email: thomas.barbarisque1@uqac.ca

⁷Professor, Département de Génie Civil et de Génie des Eaux, Université Laval, QC, G1V 0A6, Canada. Email: jean-pascal.bilodeau@geci.ulaval.ca

Abstract

In recent years, permafrost warming has adversely affected the performance of infrastructure projects existing in northern Canada. The common construction practice in these permafrost-underlain areas is to prefer the use of the pile foundation for building and infrastructure rather than using shallow foundations. Thus, the influence of warming permafrost on the loading capacity of pile foundations is critical for evaluating forthcoming changes under a warming climate. The present study was performed to assess the influence of temperature and loading rate on the adfreeze strength of piles in permafrost soil. A series of uniaxial compressive tests on wooden piles drilled into frozen soil were carried out at various temperatures, mimicking the conditions in warming permafrost. The results demonstrated that

an increase in strain rate led to an increase in adfreeze strength of piles. Moreover, the wooden piles exhibited peak adfreeze strength at a displacement less than 2 mm for most temperature and deformation rate combinations. Interestingly, although the adfreeze strength of piles increased as temperatures cooled below $-1\text{ }^{\circ}\text{C}$, a transition phase between -3 and $-4.5\text{ }^{\circ}\text{C}$ was observed in which the adfreeze strength decreased. It can be noted that failure occurred in the wooden piles at temperatures colder than $-5\text{ }^{\circ}\text{C}$ rather than frozen soil failure at these temperatures. These variations in adfreeze strength are related to soil temperature, unfrozen water content, and the adhesive bonds at the interface between the frozen soil and pile.

Keywords: Adfreeze strength, permafrost, strain rate, temperature, wooden piles

INTRODUCTION

Over the past few decades, a marked increase in population and economic development in the high-latitude regions of North America has heightened the need for geotechnical engineers to provide safe and cost-effective infrastructure design in these cold-climate regions underlain by permafrost. Permafrost is ground that remains at or below $0\text{ }^{\circ}\text{C}$ for at least two consecutive years (Bordignon 2021). Over the last 20 years, Arctic surface air temperature has increased by more than double the global average, and the near-surface permafrost in the Arctic has warmed by more than $0.5\text{ }^{\circ}\text{C}$ between 2009 and 2017 (Biskaborn et al. 2019), triggering permafrost thaw. With climate warming and changes in the snow regime, the temperature of the permafrost soils has also warmed, the seasonal thaw period has lengthened, and the degradation of permafrost has accelerated, accompanied by an altered extent of permafrost distribution (Nikiforova and Konnov 2021). Climate warming causes altering the depth, distribution, engineering behavior of permafrost and subsequent degradation of permafrost has led to differential settlement of infrastructure leading to considerable damage to installations and increased economic costs (Alfaro et al. 2009; Li et al. 2016; Wang et al. 2014; You et al. 2017). For example, airstrips built by the Quebec Ministry of Transport in the permafrost regions of northern Quebec began

to exhibit signs of major settlement, creep, and longitudinal cracking only a few years after their construction because of changes in the active layer and permafrost behavior (Bilodeau et al. 2019). Similarly, the Alaska Highway, which links northern British Columbia to Alaska, has shown signs of road damage induced by permafrost degradation (Stephani et al. 2014). Even though a significant amount of research has focused on assessing permafrost and its behavior as foundation material, the changed climatic conditions with projections of future warming necessitate an improved understanding of permafrost behavior under changing conditions to aid ongoing and future development of infrastructure in circum-Arctic regions. Multiple infrastructure construction projects such as public buildings, large diameter pipelines, drilling platforms, mining facilities, power transmission lines, highways, bridges, railway lines, and telecommunication lines are currently underway in the permafrost regions of northern Canada. While spread footings, column footings, continuous footings, and raft or mat foundations have satisfied the stability requirements of buildings and structures constructed on permafrost, they cannot ensure structural longevity because of permafrost thaw of the upper soil layers (Verreault 2015).

Pile foundations are considered one of the most progressive and economic types of foundations to support infrastructure even in warm permafrost (Tang et al. 2019). For example, the Inuvik to Tuktoyaktuk Highway project used steel pipe piles as a foundation for eight bridge crossings where the 140 km route consists of continuous permafrost with ground temperatures ranging between -1.8 to -4.3 °C (Hoeve and Fortin 2019). The capacity of single piles in permafrost subjected to static axial loads is controlled by the load-settlement rate and is predominantly affected by permafrost temperature profile at the site (Andersland and Ladanyi 2013). Early studies have indicated that around 80% of the bearing capacity of pile foundations in permafrost is provided by interface shear resistance between the pile material and permafrost soil and only 10% to 20% of bearing capacity relates to the end bearing, which is typically excluded from design considerations (Aksenov and Kistanov 2008; Targulyan and Bashkirov 1987). The adfreeze bond, synonymous with interface shear resistance of

piles in permafrost, contributes to the bearing capacity of piles in permafrost and has been the major focus of research. Parameswaran (1981) evaluated the influence of pile material on adfreeze strength of permafrost over a temperature range of -6 to -10 °C and suggested that the adfreeze strength of wood and steel increases linearly with an augmented rate of displacement. Landanyi and Guichaoua (1985) evaluated bearing capacity of different types of friction piles in permafrost under constant loading and strain rates, finding that smooth, straight shafted piles fail in a brittle manner at strains beyond peak shear stress. Aksenov and Kistanov (2008) demonstrated that the long-term variation of shear resistance of friction piles in saline permafrost depends on temperature and unfrozen water content. Similarly, Scarr and Mokwa (2008) determined the axial capacity of timber piles in permafrost and highlighted the importance of freezing temperature on adfreeze strength. Moreover, Semi-empirical, empirical, numerical, and analytical relationships have been developed to determine bearing capacity and the settling of piles in frozen soil; for example, Jiang and Guo (2016) numerically simulated the long-term bearing capacity of an in-situ concrete pile in permafrost in Tibet.

Although existing studies considered various factors that influence the adfreeze strength/ bearing capacity of piles in permafrost, only recently has research begun to investigate climate change on the performance of piles in permafrost (Aldaef and Rayhani 2018; Hoeve and Fortin 2019; Tang et al. 2019). Aldaef and Rayhani (2018) evaluated the adfreeze strength and creep behavior of steel piles in warming permafrost (temperatures ranging from -3 to 0 °C) and illustrated that the pile in warm permafrost fail in brittle mode post-peak strength because of permafrost degradation. Tang et al. (2019) investigated the axial loading behavior of laboratory concrete piles in permafrost silt and clay at a ground temperature of -1.10 to -2.35 °C and found that adfreeze strength had not been mobilized near the pile tip because the axial load transferred to the pile tip was insufficient. This reflects the scarcity of scientific literature pertaining to the impact of changing climatic conditions on the capacity of piles constructed in permafrost at a temperature range between 0 °C and -5 °C. In light of the ongoing infrastructure construction in warming permafrost regions of northern Canada, the present

study seeks to investigate the influence of varying temperatures and strain rates on the adfreeze/interface shear resistance between the pile and frozen clay.

DESIGN OF LABORATORY MODEL TESTS

Laboratory model tests on wooden piles were performed to determine the adfreeze strength of piles subjected to compression in permafrost regions. Compression tests on model piles were carried out in the atmospheric icing center at the Université du Québec à Chicoutimi (UQAC). We developed a methodology for determining the frictional capacity of the pile in the permafrost soil (Fig. 1). This study simulated the soil profiles and permafrost temperatures of sites in northern Canada.

Laboratory soil and model pile properties

Representative samples of typical northern Canadian permafrost soil were prepared by combining various regional clays found across Quebec. The field moisture content of the soil varied between 25% and 30%. According to USCS classification, the soil used in the investigation was a low plastic silty clay with traces of fine sand (CL) which had a liquid limit of 44% and a plasticity index of 19. Fig. 2 depicts the grain size distribution of soil determined in accordance with ASTM D 422 (2003).

Smooth solid wooden piles of untreated birch wood having an average diameter of approx. 24.75 mm and an interaction length of approx. 80 mm were employed in this investigation (Fig. 3). Although untreated wooden piles comprised of spruce, larch, Douglas fir, and jack pine are most preferred in northern Canada (Ruddick 2018), the present study selected piles made of birch because of their availability in the study area and the ease of preparing model piles with this wood species. Birch wood is classified as low durability class relative to other preferred woods such as spruce, larch, Douglas fir, and jack pine; however, the engineering properties of all these wood types are similar (Johansson et al. 2013).

Preparation of wooden pile – permafrost soil model

The development of wooden pile – permafrost soil model involved preparing the soil in a 100-mm-diameter plexiglass mold with a height of 100 mm (Fig. 3). The height of the soil model was fixed as 80 mm with each compacted soil lift thickness of about 27 mm. Proper care was taken throughout the model soil preparation to achieve and maintain a soil moisture content like that observed in the field. All samples were prepared identically, and fresh soil was used to prepare each soil model (Fig. 3). As the behavior of permafrost is very temperature dependent, accurate temperature assessment is crucial to ensure the validity of the results. The temperature of the permafrost soil model was measured using type K sensors having an accuracy of ± 0.05 °C and placed into the soil in holes created using a 3 mm drill bit (Fig. 4). The soil model was then kept frozen at the atmospheric icing center for 48 hours at -10 °C. The -10 °C temperature was selected because at higher temperatures the soil became too soft to install the pile without failure of the soil model. After freezing the soil model, the holes were drilled in the soil to place the model piles to construct a wooden pile-permafrost soil model.

In Canada, the widespread practice for installing piles into permafrost is to drill a pilot hole slightly larger than the pile, insert the pile, and then fill the excess space with sand and water slurry (Government of Quebec 2018). In this study, the model pile was placed into an 80-mm-deep, 25-mm-diameter drill hole in the permafrost soil model. A drill bit was used to produce the hole, and proper care was taken to ensure that the drill bit did not affect the permafrost soil model during the installation of the model pile. A soil–water slurry filled the annular space between the wooden pile and soil. An additional flexible bending sensor is introduced at 10 mm from the permafrost soil model surface to evaluate the presence of any bending movements within the sample during the tests (Fig. 4). The sensor was inserted into the permafrost soil model at a temperature of -10 °C. The wooden pile–permafrost soil model with the sensor assembly was then kept at the required experimental temperatures (-1 to -5 °C) for 48 h in the atmospheric icing center. This approach ensured that the entire permafrost soil

model was monolithic and that its behavior was very similar to that of polycrystalline ice (Ladanyi and Theriault 1990).

Instrumentation system design

Simple axial compression tests were carried out in the laboratory of the atmospheric icing center at the Université du Québec à Chicoutimi. This laboratory allows air temperatures to vary between $-6\text{ }^{\circ}\text{C}$ and $0\text{ }^{\circ}\text{C}$. For the testing, an *MTS 810* machine fitted with a 25 KN loading cell (Model 661.20E-01) was used. A plate placed on top of the pile was designed to ignore resistance at the pile head and measure only axial shear within the sample. The plate design prevented the pile head from producing any resistance during the test (Fig. 5a). The plate also contained a lateral opening for inserting a 7 mm micro-endoscopic camera (Fig. 5b) to visually record the alignment and displacement of the pile. This visual record ensured that any observed friction was not produced by the friction of the pile with the seat plate, and it allowed for verifying that pile travel was sufficient.

Testing procedure

The axial compression tests were performed for several loads at $1\text{ }^{\circ}\text{C}$ intervals between -1 and $-5\text{ }^{\circ}\text{C}$ (note that the tests carried out at $-6\text{ }^{\circ}\text{C}$ caused the breakage of the piles). A deviation of around $\pm 0.3\text{ }^{\circ}\text{C}$ was observed during testing in the cold room chamber for a specified test temperature. For each temperature, tests were performed at three deformation rates: 0.01, 0.1, and 0.5 mm/s, and all tests were repeated three times. The axial stresses and strains were measured during the tests. A linear variable differential transformer (LVDT) sensor was installed to determine the displacement of the monolithic soil. The axial displacement of the acquisition head and the LVDT sensor ($\pm 0.05\text{ mm}$) differed by 0.002 mm. This displacement is attributed to the seating of the material and not to the displacement of the pile in the clay. Therefore, this displacement is disregarded in the interpretation of the results. Displacement was determined as

$$\Delta_{\text{absolu}} = (D_{\text{press}} + D_{\text{LVDT}}) - (P_{\text{initial, press}} + P_{\text{initial, LVDT}}) \quad \dots\dots\dots(1)$$

where Δ_{absolu} represents the actual displacement between the pile and the clay, D_{press} is the press displacement pressed on the pile, D_{LVDT} is the displacement of the LVDT sensor located on the clay, and $P_{\text{initial, press}}$ and $P_{\text{initial, LVDT}}$ are the initial press position and initial LVDT position, respectively (Fig. 6). The maximum shaft resistance of the wooden pile in permafrost clay was obtained from the ratio of maximum axial force to the surface area corresponding to the corresponding displacement of the pile.

RESULTS AND DISCUSSION

The results of the axial compression tests at varying temperatures and strain rate of 0.01 mm/s are shown in Fig. 7. The ultimate shear stress (which is obtained by dividing the axial load by the surface area of pile in contact with permafrost) is assigned to the vertical axis and the axial displacement is plotted on the horizontal axis. The ultimate shear stress-displacement curves for all the tests on piles at other deformation rates with various temperatures ranging between 0 to -5 °C are depicted in Figs. 8-9. From Fig. 7, it was found that, at a strain rate of 0.01 mm/s and -1 °C, the adfreeze strength was about 297 kPa. The adfreeze strength increased to about 634 kPa and 854 kPa at -2 °C and -3 °C respectively, whereas it decreased to about 258 kPa at -4 °C. At -5 °C, the adfreeze strength again increased to about 1146 kPa. It was observed that the adfreeze strength at -5 °C was almost 4 times at -1 °C. Even at strain rates 0.05 and 0.1 mm/s (Figs. 8-9), adfreeze strength increased as temperatures cooled from -1 to -3 °C. At -4 °C, the adfreeze strength was lower than that for -1 to -3 °C but then increased to reach a maximum value at -5 °C. At -4 °C test temperature, the soil-pile model failed in a plastic manner with a comparatively smaller difference between peak and residual shear stress. At all remaining test temperatures, the soil-pile model exhibited brittle failure with a pronounced difference between peak and residual shear stress. The decrease of adfreeze strength of wooden piles between -3 °C and -5 °C for all three deformation rates seemed anomalous. Tests were conducted between -3 °C and -4 °C temperatures to establish the decrease in adfreeze strength

between the temperature range of -3 to -5 °C for all strain rates whereas the strain rate corresponding to 0.01 mm/s was depicted in Figure 10 as an example. In Fig. 10, T1, T2, T3, T4, and T5 represent the number of trails at each temperature. As depicted in figure 10, the overall results show a scatter between -3 °C and -4 °C temperatures. For each specific temperature, the scatter is trivial in terms of peak stress/strength. The accuracy of the repeated experiments at each specified temperature is justified by the temperature precision of 0.1 °C in the atmospheric icing centre. Additionally, all tests showed similar trends (Fig. 11) and confirmed a reduction in adfreeze strength between -3 to -5 °C regardless of the applied strain rate.

Variation in the adfreeze strength of the soil-pile model occurs because the adfreeze strength at the wooden pile–frozen soil interface arises through the combination of adhesion between the ice–pile surface and soil–pile interface. When the temperature reduces to below 0 °C, some of the available free water in soil pores partially freezes, whereas the remaining water remains unfrozen (Fig 12a). The fraction of unfrozen water is high at -1 °C and it decreases as the temperature reduces to -3 °C. This decrease of unfrozen water (in other words increase of partially frozen water) enhances the adhesive bonds between partially frozen soil and wooden piles, thereby enhancing the adfreeze strength. However, at temperatures cooler than -3 °C temperature, supercooling occurs, characterized by the triggering of partially frozen pore water into ice transformation with a small transient increase in temperature (Shah and Mir 2022). This supercooling—dependent on soil gradation, mineralogy, and unfrozen water content—occurs in a metastable state present only at the initiation of ice nucleation and should not be confused with freezing-point depression. During this temperature range between -3 and -4.5 °C, the rate of reduction of unfrozen water content is almost trivial for fine-grained silty clays (Anderson and Tice 1972, Tsytovich and Sumgin 1959). The reduced adfreeze strength between -3 °C and -4.5 °C can be attributed to this supercooling. Subsequently, at temperatures cooler than -5 °C, the ice nucleation reaches its maximum, and the adhesive bond between the interface of ice-coated/lensed soil and pile increases considerably causing a significant increase in the adhesive bond.

Furthermore, in most cases, the failure was observed in the wooden piles rather than frozen soil (Fig 12b). Following cracking, the stress is taken up entirely by adfreezing, testifying that the admissible lateral shear strength of a pile is equal to that of the adfreeze strength. At $-6\text{ }^{\circ}\text{C}$, the destruction of the wooden piles was observed with stresses exceeding 2200 kPa. Ice strength exceeding 2000 kPa at temperatures less than $-5\text{ }^{\circ}\text{C}$ was also reported by Farid et al. (2016); this stress provoked the failure of wooden piles rather than the frozen soil. Ladanyi and Theriault (1990) also highlighted the poor structural capacity of wooden piles though these piles exhibit good insulation properties and relatively high bond strength. The adfreeze strength computed in the present study was considerably higher than that reported by Aldaeef and Rayhani (2018) and lower than that found by Tang et al. (2019) for the same temperature range. These discrepancies may be attributed to differences in testing conditions.

Experimental results clearly demonstrate that the temperature has a clear and significant impact on the adfreeze strength of the frozen soil. As the strain rate increased, the adfreeze strength increased at all studied temperatures. It is evident from all shear stress-displacement curves that the adfreeze strength reaches a maximum value, corresponding to peak adfreeze strength, followed by a decrease and eventual plateau, which marks the residual adfreeze strength. The significant reduction of adfreeze strength post-peak value indicates the brittle failure mode, which can be attributed to the viscoelastic behavior of frozen soil. The residual strength after the failure of the adfreeze relates mainly to friction. In addition to that, for nearly all combinations of temperature and deformation rate, the wooden piles exhibited peak adfreeze strength at a displacement less than about 2 mm followed by very less post-peak adfreeze strength. A similar observation of failure of smooth piles at low stress in a brittle manner after a displacement of around 2 mm in permafrost was reported by Ladanyi and Guichaoua (1985). It would have been interesting to produce the recovery of adfreeze strength and then repeat the test. However, this test would require no movement of the seat plate during the test and an accuracy of $0.01\text{ }^{\circ}\text{C}$ during the entire duration of recrystallization.

Limitations of the study

Our research focused on the assessment of adfreeze frictional strength of a wooden birch pile in warm permafrost soil. Nonetheless, other materials, such as steel, concrete, and other preferred woods require similar testing, as they do not act the same in warm permafrost soils. Moreover, the reported adfreeze strength variations in warm permafrost soil are based solely on experiments undertaken using low-plastic clay. Therefore, the reported behavior is applicable for similar types of wooden piles and soils, whereas the characteristics of soils used in specific field conditions will differ perpetually. Future experiments should also include creep tests, which are critical for frozen soils and necessary for predicting the time-dependent settlement of a pile. Finally, an assessment of the scale effect between laboratory and field results is required to build a comprehensive model of pile design in high-latitude regions underlain by warm permafrost.

CONCLUSIONS

The objective of the work was to assess the adfreeze strength of model wooden piles installed in frozen soil through systematic laboratory compression tests at various temperatures and strain rates. The following conclusions can be drawn based on the analysis of results:

1. Adfreeze strength increased as the deformation rate increased for all temperatures between -1 °C and -5 °C with a transition phase between -3 to -4.5 °C. Adfreeze strength increased fourfold as temperatures cooled from -1 to -5 °C.
2. For most temperature and deformation rate combinations, the wooden piles exhibited the highest adfreeze strength at a displacement less than about 2 mm.
3. Enhanced adfreeze strength can be attributed to adhesive bonds between partially frozen soil and wooden piles at -1 to -3 °C. Supercooling phenomenon present at the initiation of ice nucleation with a small transient increase of temperature within the frozen soil led to a decreased adfreeze strength between -3 °C and -4.5 °C.

4. The higher adfreeze strength at -5°C is attributed to the increased adhesive bond between the interface of ice coated/lensed soil and pile caused by ice nucleation. The wooden pile failed at -6°C as the stresses within the pile exceeded 2200 kPa.

These results will help to improve the infrastructure design adapted to the changing permafrost environment in northern Canada and other circum-Arctic regions.

DATA AVAILABILITY STATEMENT

All data, models, and code generated or used during the study appear in the submitted article.

ACKNOWLEDGMENTS

The authors would like to thank the organizations that have funded this project: Natural Sciences and Engineering Research Council of Canada (Grant No. RGPIN-2019-06693) and FUQAC. The authors would also like to Mrs. Maryse Doucet, Mr. David Noël, and Mr. Pierre Camirand for their collaboration during the experimental procedure.

AUTHORS' CONTRIBUTIONS

Funding acquisition, A.S.; methodology, J.M., A.S., and T.B.; project administration, A.S. and M.S.; supervision, A.S. and J.B.; writing – original draft, J.M., T.B., A.S., and R.V.; review and editing, A.S., M.S., R.V., and J.B.

COMPETING INTERESTS

The authors declare that there are no competing interests.

REFERENCES

- Aksenov, V. I., Kistanov, O. G., 2008. "Estimation of resistance components to an axial load on piles embedded in permafrost". *Soil Mechanics and Foundation Engineering*, 45(2): 71-75.
- Aldaef, A. A., Rayhani, M. T., 2018. "Adfreeze strength and creep behavior of pile foundations in warming permafrost". In: *Advances in analysis and design of deep foundations*, 254-26. GeoMEast 2017. Sustainable Civil Infrastructures. Springer, Cham. https://doi.org/10.1007/978-3-319-61642-1_20
- Alfaro, M. C., Ciro, G. A., Thiessen, K. J., Ng, T., 2009. "Case study of degrading permafrost beneath a road embankment". *Journal of Cold Regions Engineering*, 23(3) : 93-111.
- Andersland, O. B., Ladanyi, B., 2013. "An introduction to frozen ground engineering". *Springer Science & Business Media*. <https://doi.org/10.1007/978-1-4757-2290-1>
- Anderson, D. M., Tice, A. R., 1972. "Predicting unfrozen water contents in frozen soils from surface area measurements". *Highway research record*, 393(2): 12-18.
- Bilodeau, J. P., Verreault, J., Doré, G., 2019. "Assessment of the physical and mechanical properties of permafrost in Nunavik, Quebec, Canada". In: *Cold Regions Engineering*, 17-25. Reston, VA: American Society of Civil Engineers.
- Biskaborn, B. K., Smith, S. L., Noetzli, J., Matthes, H., Vieira, G., Streletskiy, D. A., ... Lantuit, H., 2019. "Permafrost is warming at a global scale". *Nature communications*, 10(1): 1-11.
- Bordignon, F., 2021. "A scientometric review of permafrost research based on textual analysis (1948–2020)". *Scientometrics*, 126(1) : 417-436.
- Government of Quebec, 2018. "Housing construction in Nunavik: Guide to good practices." *Société d'habitation du Québec (SHQ)*, Quebec, Canada.
- Farid, H., Farzaneh, M., Saeidi, A. and Erchiqui, F., 2016. "A contribution to the study of the compressive behavior of atmospheric ice". *Cold Regions Science and Technology*, 121: 60-65.
- Hoeve, T. E., Fortin, B., 2019. "Adfreeze pile design for bridges along the Inuvik to Tuktoyaktuk Highway, Northwest Territories". In: *Cold Regions Engineering*, 406-414. Reston, VA: American Society of Civil Engineers.
- Jiang, D. J., Guo, C. X., 2016. "Long-term stability of bearing capacity of single pile in permafrost area on Qinghai-Tibetan Plateau". *Journal of Chang'an University*, 36(2) : 59-65.
- Johansson, M., Säll, H. and Lundqvist, S.O., 2013. *Properties of materials from Birch—Variations and relationships: Part 2. Mechanical and physical properties*. Linnaeus University.
- Landanyi, B., Guichaoua, A., 1985. "Bearing capacity and settlement of shaped piles in permafrost". In: *International Conference on Soil Mechanics and Foundation Engineering*. 11: 1421-1427.

- Ladanyi, B., Theriault, A., 1990. "A study of some factors affecting the adfreeze bond of piles in permafrost". *In Proc. of Geotechnical Engineering Congress GSP*, 27: 213-224.
- Li, G., Yu, Q., Ma, W., Chen, Z., Mu, Y., Guo, L., Wang, F., 2016. « Freeze–thaw properties and long-term thermal stability of the unprotected tower foundation soils in permafrost regions along the Qinghai–Tibet Power Transmission Line”. *Cold Regions Science and Technology*, 121: 258-274.
- Nikiforova, N. S., Konnov, A. V., 2021. "Influence of permafrost degradation on piles bearing capacity". *In Journal of Physics: Conference Series*, 1928(1), p. 012046. IOP Publishing.
- Parameswaran, V. R., 1981. "Adfreeze strength of model piles in ice". *Canadian Geotechnical Journal*, 18: 8–16.
- Ruddick, J.N., 2018. "Performance of Treated Wood in the Arctic". *In Proceedings of the Canadian Wood Preservation Association 39th Annual Meeting*, Vancouver, Canada, pp. 17-24.
- Scarr, K. L., Mokwa, R. L., 2008. "Axial capacity of piles founded in permafrost: A case study on the applicability of modern pile design in remote Mongolia". *In Proceedings of 41st Symposium on Engineering Geology and Geotechnical Engineering*, pp. 51-66.
- Shah, R. and Mir, B. A., 2022. "The Freezing Point of Soils and the Factors Affecting its Depression". *In Advances in Construction Management*. Springer, Singapore, pp. 157-166.
- Stephani, E., Fortier, D., Shur, Y., Fortier, R., Doré, G., 2014. "A geosystems approach to permafrost investigations for engineering applications, an example from a road stabilization experiment, Beaver Creek, Yukon, Canada". *Cold Regions Science and Technology*, 100: 20-35.
- Tang, L., Wang, K., Deng, L., Yang, G., Chen, J., Jin, L., 2019. "Axial loading behaviour of laboratory concrete piles subjected to permafrost degradation". *Cold Regions Science and Technology*, 166, 102820.
- Targulyan, Y. O., Bashkirov, V. M., 1987. "Characteristic features of the embedment of steel-tube piles in permafrost of the Tyumen Oblast". *Soil Mechanics and Foundation Engineering*, 24(3) : 92-95.
- Tsytovich, N. A., Sumgin, M. I., 1959. "Principles of mechanics of frozen ground". *Cold Regions Research and Engineering Lab Hanover NH*.
- Verreault, M. J., 2015. "Caractérisation du pergélisol et stratégie d’adaptation pour les aéroports du Nunavik". Quebec City.
- Wang, G. S., Yu, Q. H., You, Y. H., Zhang, Z., Guo, L., Wang, S. J., Yu, Y. 2014. "Problems and countermeasures in construction of transmission line projects in permafrost regions". *Sciences in Cold and Arid Regions*, 6(5) : 432-439.

You, Y., Wang, J., Wu, Q., Yu, Q., Pan, X., Wang, X., Guo, L., 2017. "Causes of pile foundation failure in permafrost regions: The case study of a dry bridge of the Qinghai-Tibet Railway". *Engineering Geology*, 230 : 95-103.

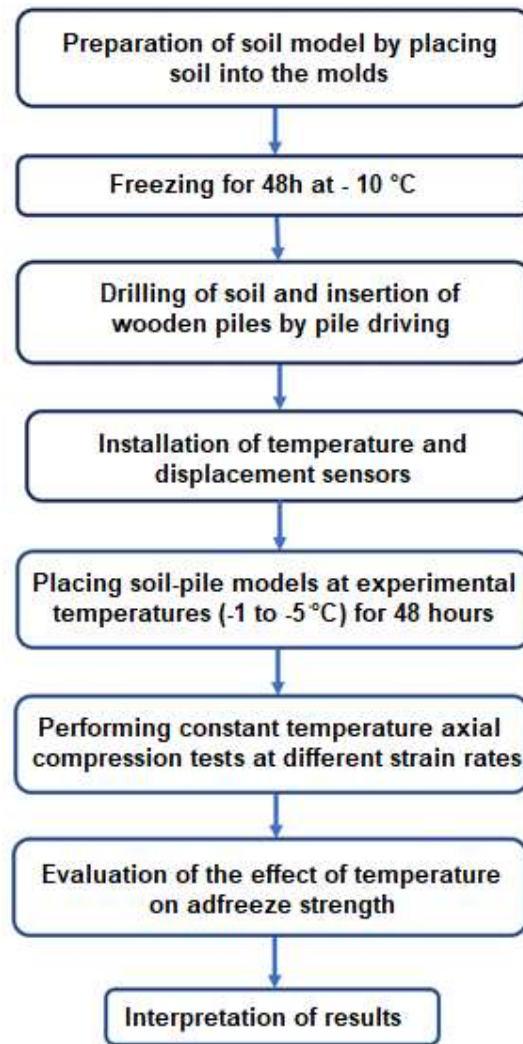
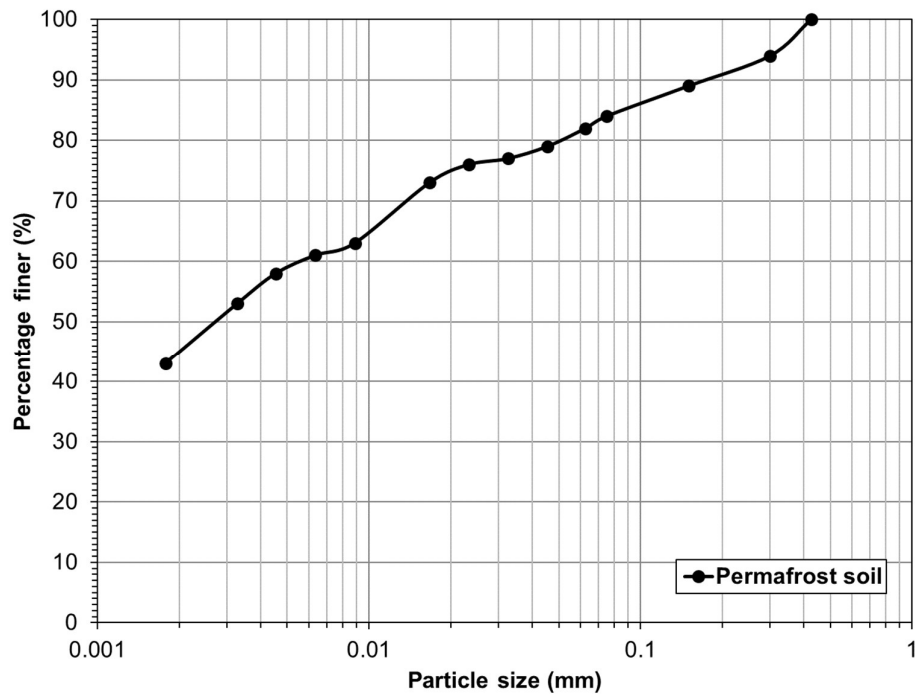


Fig. 1. Methodology for determining the bearing capacity by lateral friction of a wooden pile in permafrost at various temperatures and loading rates.



(a) (b)
Fig. 2. Soil details a) grain size distribution of soil and b) soil samples ready for freezing.

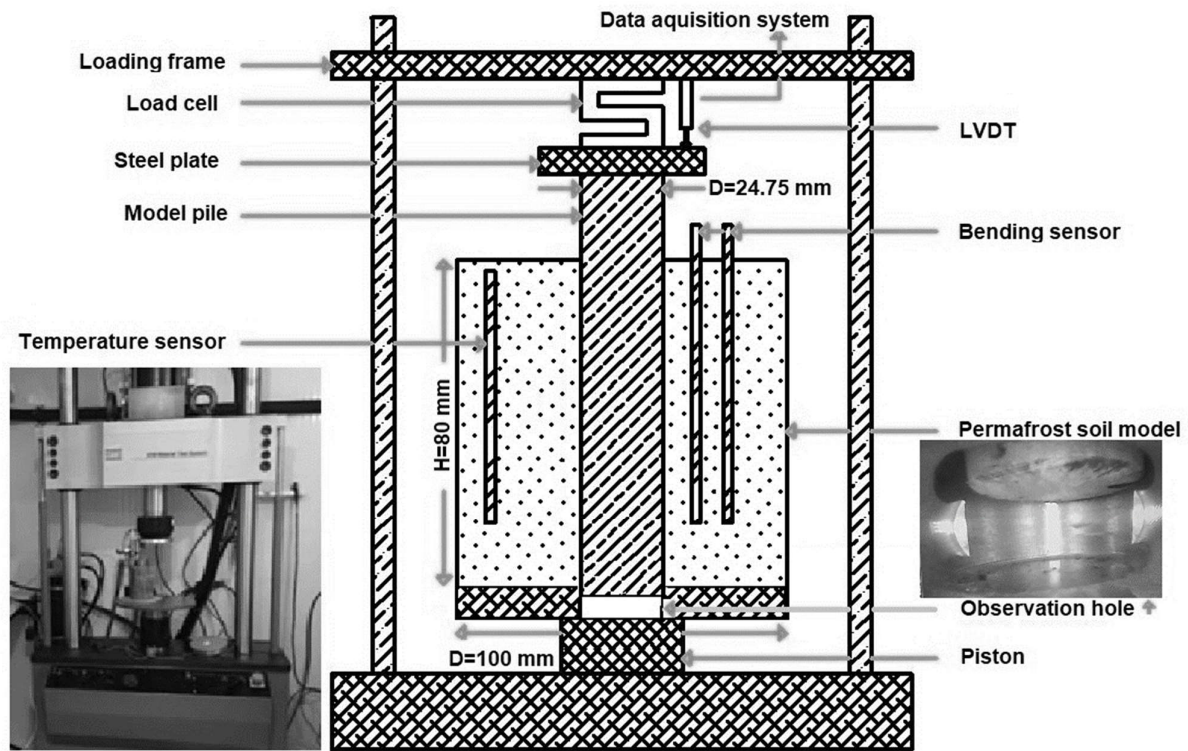
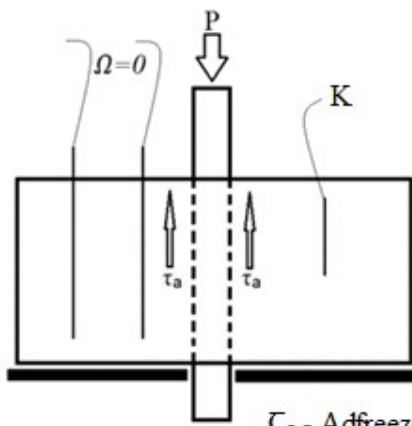


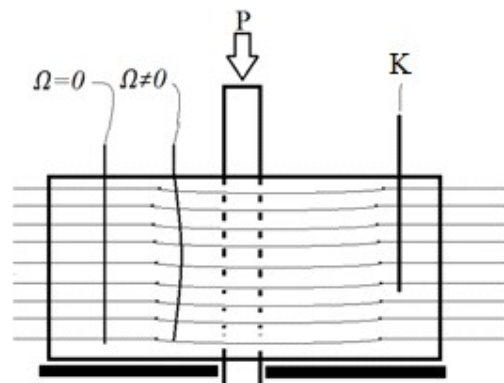
Fig. 3. Schematic diagram of the laboratory permafrost soil – wooden pile model test setup



(a)



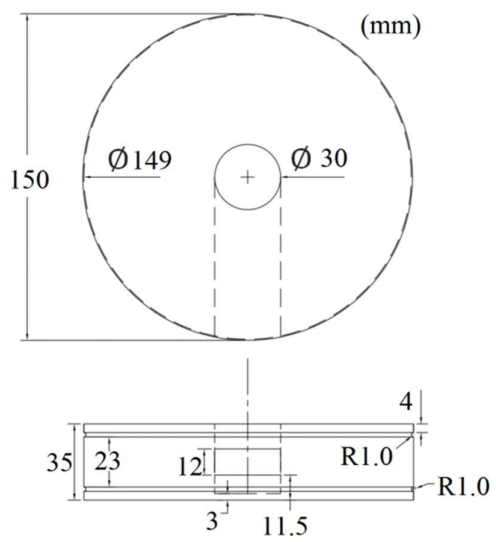
τ_a - Adfreeze strength
 P - Axial load



K - Type of sensor
 Ω - Deflection sensor

(b)

Fig. 4. a) Photos of the bending sensor (right) and its placement in the soil (left). b) Position of sensors (left) and the zones of influence using bending gauges (right).



(a)



(b)

Fig. 5. a) Modified plate for carrying out the test. b) Image of the pile head camera window.

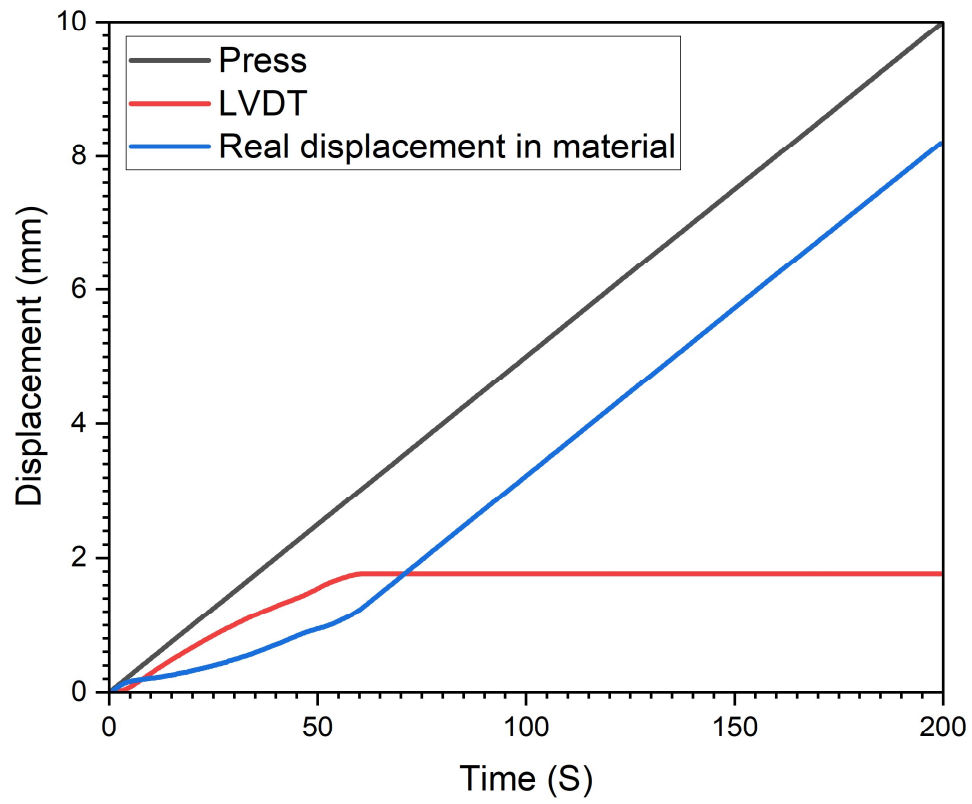


Fig. 6. Displacement between the pile and the clay over time.

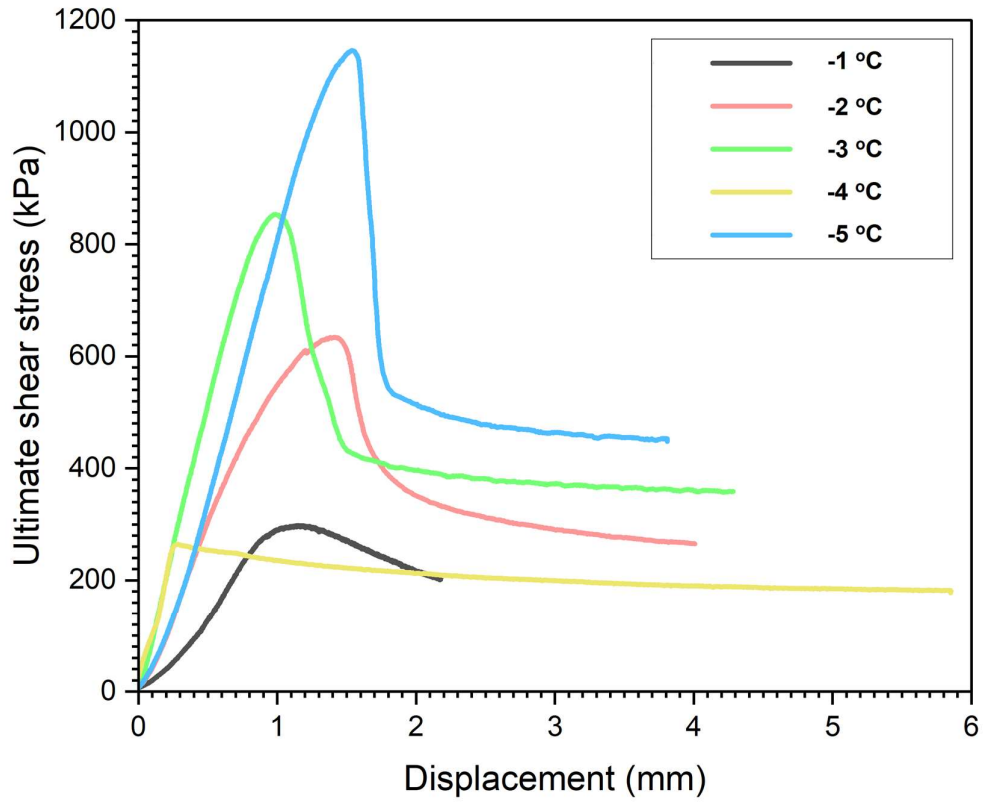


Fig. 7. Shear stress-displacement curves at various temperatures under strain rate of 0.01 mm/s

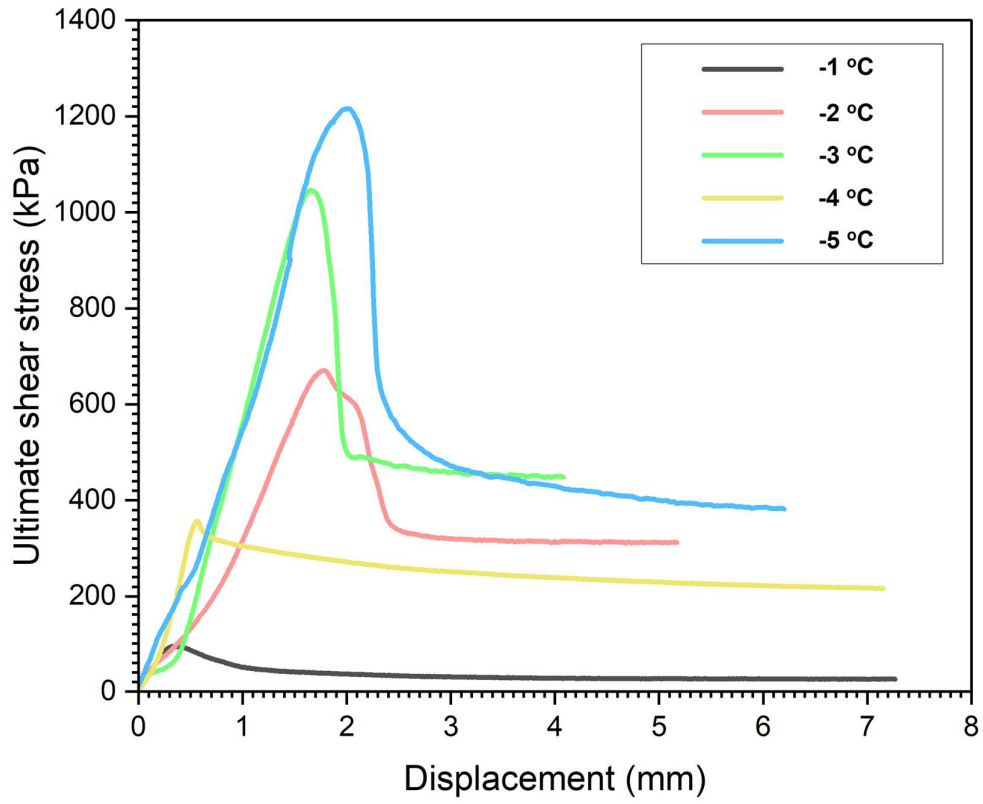


Fig. 8. Shear stress-displacement curves at various temperatures under strain rate of 0.05 mm/s

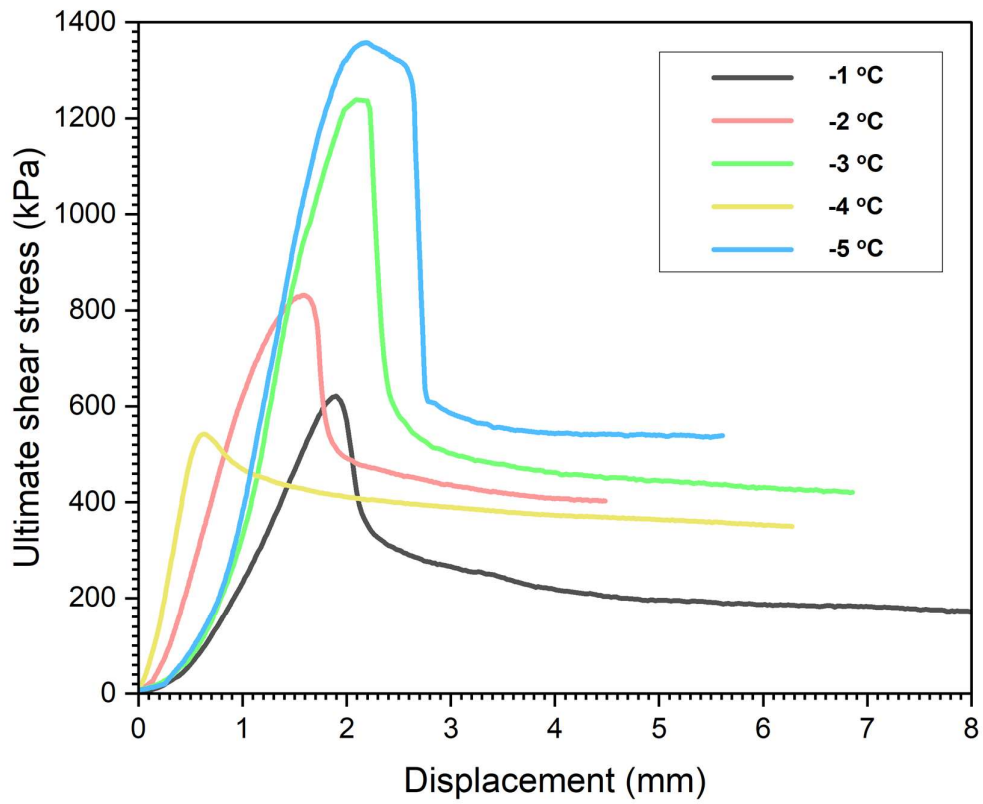
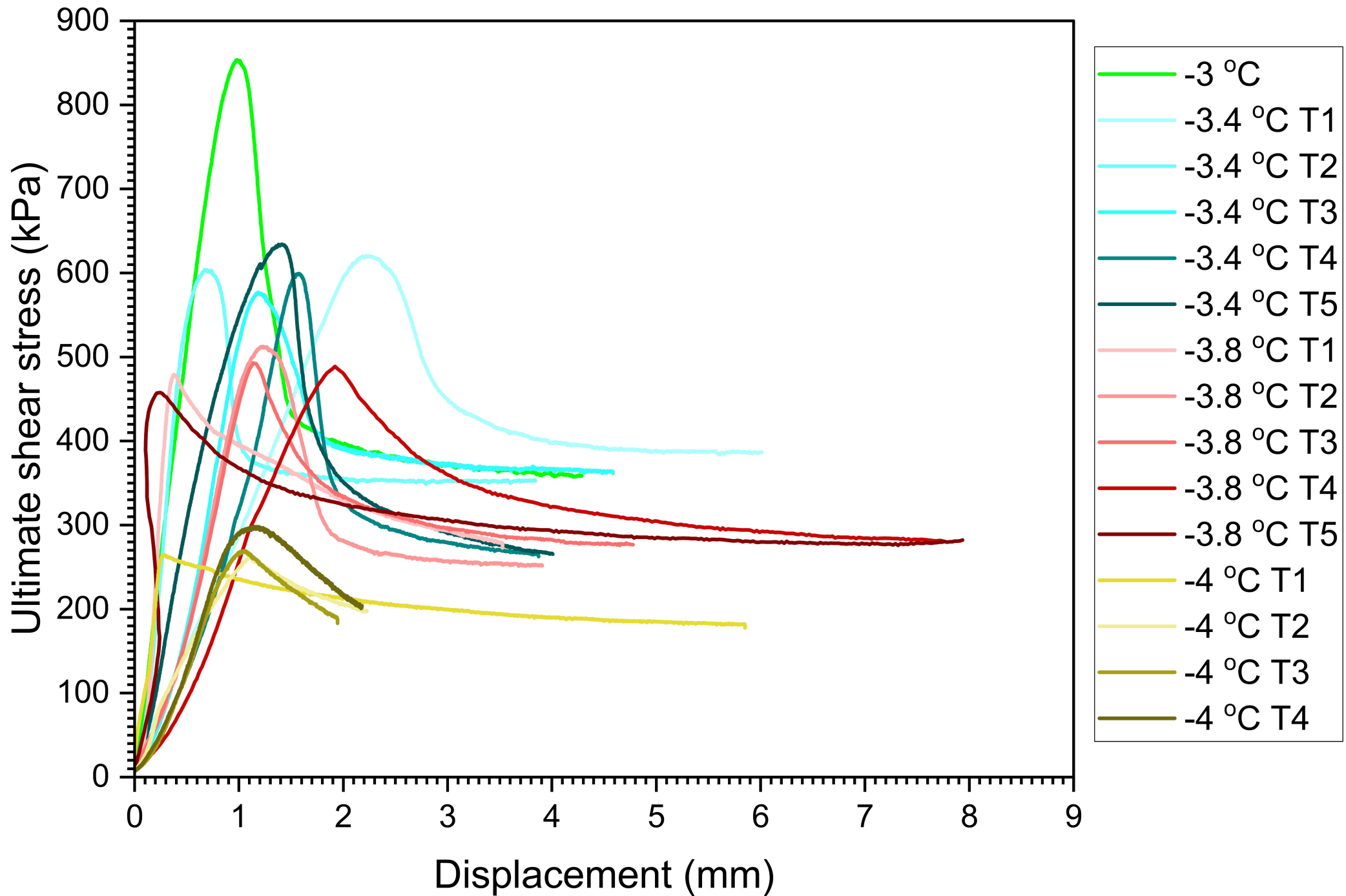


Fig. 9. Shear stress-displacement curves at various temperatures under strain rate of 0.1 mm/s



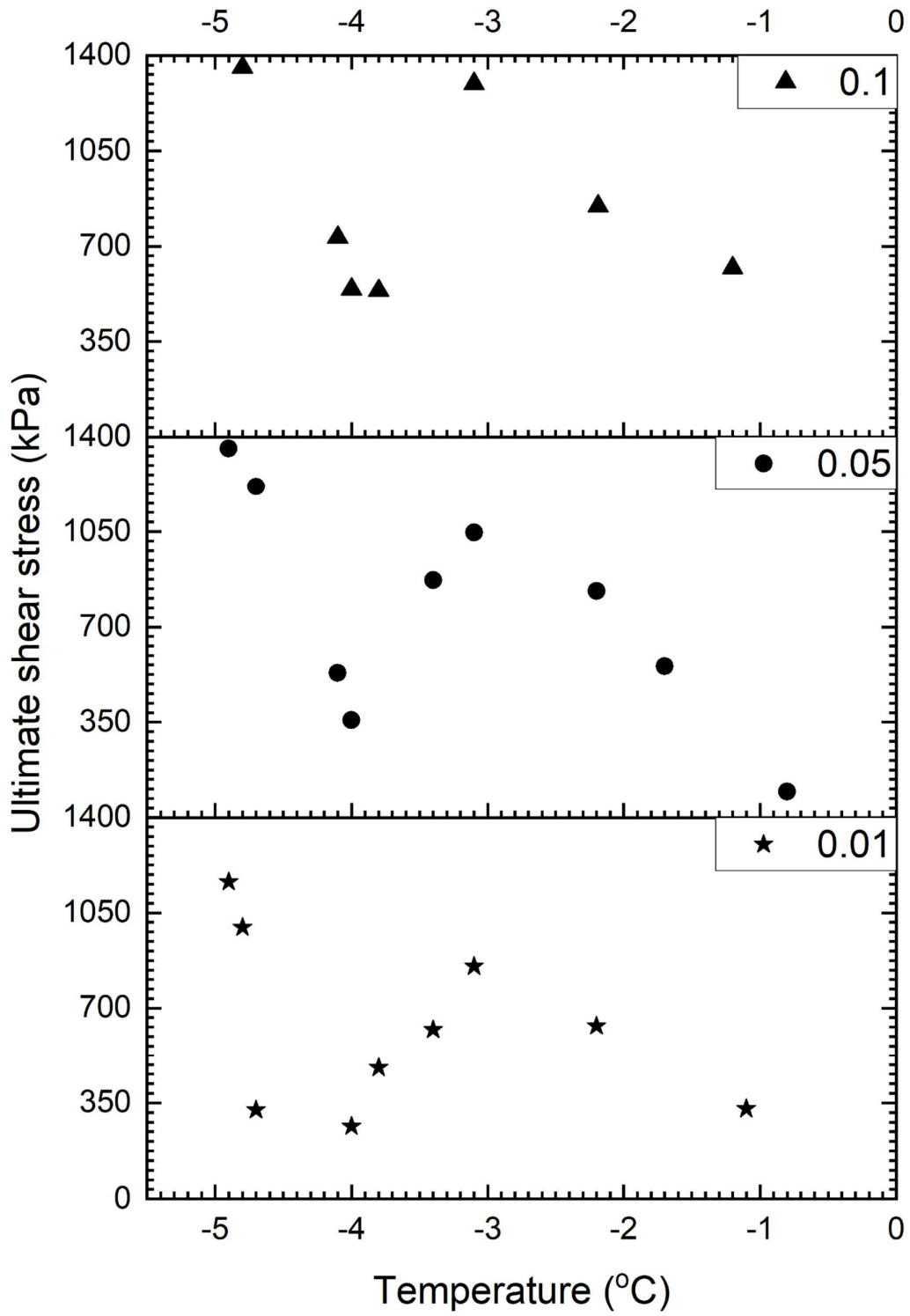


Fig. 11. Relationship between ultimate shear stress and soil temperatures at various strain rates.



(a) (b)
Fig. 12. a) Water at $-1\text{ }^{\circ}\text{C}$ with the presence of liquid. b) Apparent significant cracking for tests at $-5\text{ }^{\circ}\text{C}$ (center) and $-4\text{ }^{\circ}\text{C}$ (right).